


PRDM4 mediates YAP-induced cell invasion by activating leukocyte-specific integrin β 2 expression

Huan Liu^{1,†}, Xiaoming Dai^{1,†}, Xiaolei Cao^{1,†}, Huan Yan¹, Xinyan Ji¹, Haitao Zhang¹, Shuying Shen¹, Yuan Si¹, Hailong Zhang², Jianfeng Chen², Li Li³, Jonathan C Zhao⁴ , Jindan Yu⁴, Xin-Hua Feng¹ & Bin Zhao^{1,*}

Abstract

Yes-associated protein (YAP) is a transcriptional co-activator and a major effector of the Hippo pathway that promotes cell proliferation and stemness, while inhibiting apoptosis. YAP plays a central role in organ size control, and its deregulation strongly promotes cancer initiation and progression. However, the mechanisms by which YAP promotes cell invasion and metastasis are not fully understood. Here, we report that YAP induces leukocyte-specific integrin β 2 (*ITGB2*) expression in cancer cells, thereby promoting cell invasion through the endothelium in a manner mimicking leukocytes. Through independent biochemical purification and a functional screen, we further identified PR/SET domain 4 (PRDM4) as a transcription factor interacting with the WW domains of YAP to mediate *ITGB2* expression and cell invasion. Consistently, *ITGB2* and *PRDM4* mRNA levels are significantly increased in metastatic prostate cancer. In addition, PRDM4 contributes to YAP-induced tumorigenesis possibly via mediating the expression of other YAP target genes. Our results demonstrate that YAP promotes cell invasion by inducing leukocyte-specific integrin expression, and identify PRDM4 as a novel transcription factor for YAP targets.

Keywords cell invasion; Hippo pathway; *ITGB2*; PRDM4; yes-associated protein

Subject Categories Cancer; Signal Transduction

DOI 10.15252/embr.201745180 | Received 15 September 2017 | Revised 17 March 2018 | Accepted 23 March 2018 | Published online 17 April 2018

EMBO Reports (2018) 19: e45180

Introduction

The Hippo pathway plays an evolutionarily conserved role in organ size control [1,2]. Mutations in this pathway lead to characteristic enlargement of organ size due to enhanced cell proliferation, reduced apoptosis, and expansion of tissue-specific progenitor cells.

In this pathway, the MST1/2 kinases (Hippo in *Drosophila*) in association with an adaptor protein SAV1 (Sav in *Drosophila*) phosphorylate LATS1/2 kinases (Wts in *Drosophila*). LATS1/2 associate with another adaptor protein MOB1A or MOB1B (collectively referred to as MOB below, *Drosophila* Mats homolog) to phosphorylate and inactivate a transcription co-activator YAP and its paralog transcriptional co-activator with PDZ-binding motif (TAZ, YAP, and TAZ are *Drosophila* Yki homologs), thus regulate gene expression [3–8].

Dysfunction of the Hippo pathway plays a key role in tumorigenesis. First, Hippo pathway genes such as *YAP*, *NF2*, and *GNAQ/GNA11* are amplified or mutated in cancers [9–12]. Second, other Hippo pathway genes, such as *SAV1*, *RASSF1A*, *MST1/2*, and *LATS1/2*, are deregulated on epigenetic and gene expression levels [13]. Third, genetic engineered mice unequivocally demonstrated a tumor suppressive role of the Hippo pathway and an oncogenic function of YAP [14–20]. Metastasis is the major reason for cancer-related mortality. The *Drosophila* Yki promotes malignant growth and invasion *in vivo* via activating a transcription factor network [21]. YAP has also been shown to promote metastasis through several mechanisms, such as triggering epithelial mesenchymal transition (EMT) [22,23], altering F-actin/G-actin turnover [24], and inhibiting anoikis [25]. However, it is unclear whether and how YAP could promote invasion of the endothelium, a key step during metastasis.

ITGB2 is an integrin subunit normally expressed only in leukocytes, in which it heterodimerizes with integrin alpha subunits to promote leukocyte adhesion to endothelium and the ensuing extravasation [26]. Here, we report that robust induction of *ITGB2* expression by YAP promotes cancer cell invasion through the endothelium, thus may help breach a key barrier in cancer metastasis. Furthermore, through two independent approaches, we identified PRDM4 as a new target transcription factor of YAP mediating *ITGB2* induction. These findings reveal a new mode of transcriptional regulation by the Hippo pathway in the context of cancer metastasis.

1 Life Sciences Institute and Innovation Center for Cell Signaling Network, Zhejiang University, Hangzhou, Zhejiang, China

2 State Key Laboratory of Cell Biology, CAS Center for Excellence in Molecular Cell Science, Institute of Biochemistry and Cell Biology, Shanghai Institutes for Biological Sciences, Chinese Academy of Sciences, Shanghai, China

3 Institute of Aging Research, Hangzhou Normal University, Hangzhou, Zhejiang, China

4 Department of Medicine-Hematology/Oncology, Robert H. Lurie Comprehensive Cancer Center, Northwestern University Feinberg School of Medicine, Chicago, IL, USA

*Corresponding author. Tel: +86 571 88208541; E-mail: binzhao@zju.edu.cn

[†]These authors contributed equally to this work

Results and Discussion

YAP induces *ITGB2* expression in cancer cells

ITGB2 is one of the most strongly induced YAP target genes in MCF10A human mammary epithelial cells [27,28]. This is surprising because the expression of *ITGB2* is restricted to leukocytes in physiological conditions. We confirmed that in several epithelial or cancer cell lines, *ITGB2* mRNA and protein levels could be induced by the expression of YAP, or its constitutively active 5SA mutant (serine to alanine mutation of all five Hippo pathway target sites; Figs 1A and B, and EV1A). Noteworthy, the fold induction of *ITGB2* is even stronger than that of *CTGF*, a well-established YAP target gene [22], in all three cell lines examined (Fig EV1B). We further examined *ITGB2* expression in cancer cells. We found that both *ITGB2* and *CTGF* expressions are relatively low in MCF10A, HCT116, A549, and HTB182 cells (Fig 1C). However, in ACHN and MDA-MB-231 cells, in which YAP is activated due to mutation of *Sav* and *NF2* [29], respectively, both *ITGB2* and *CTGF* expression levels are elevated. Glioblastoma cell line SF268 with YAP gene locus amplification also exhibits higher expression of YAP and *ITGB2*. *ITGB2* and *CTGF* levels are highest in an ovarian cancer cell line ES-2, in which YAP mRNA level is also relatively high (Fig 1C). Therefore, *ITGB2* is expressed in many cancer cell lines, and its expression correlates with *CTGF* expression and YAP activity. Furthermore, expression of small interfering RNAs (siRNAs) against YAP and TAZ efficiently decreased the mRNA and protein levels of both *CTGF* and *ITGB2* in ACHN cells (Fig 1D and E). Similar effect has been confirmed in ES-2 cells (Fig EV1C and D). However, knockdown of *Yap* in primary mouse bone marrow stromal stem cells (BMSSC) repressed *Ctgf* but not *Itgb2* expression (Fig EV1E), suggesting a species difference in *ITGB2* induction by YAP. Indeed, YAP overexpression did not induce *Itgb2* in two different mouse cell lines B16 and 3T3L1 (Fig EV1F and G). Taking together, *ITGB2* is a YAP target gene that could be induced by YAP activation in human cancer cells.

ITGB2 mediates YAP-induced cancer cell transendothelial invasion

Physiologically, *ITGB2*-containing integrins mediate transendothelial migration of leukocyte [30,31]. An intriguing possibility is that through YAP activation, cancer cells hijack this mechanism for metastasis. Flow cytometry analysis of A375 melanoma cells confirmed the effect of YAP in inducing *ITGB2* protein, which partially localizes to the plasma membrane (Fig 2A). We also examined the expression levels of four alpha subunits that could dimerize with *ITGB2*. Among *ITGAL*, *ITGAM*, and *ITGAX*, which were detectable in A375 cells, *ITGAM* and *ITGAX* mRNA levels were dramatically decreased by YAP activation through an unknown mechanism (Fig EV2A). Furthermore, the expression of active YAP mildly increased plasma membrane-localized *ITGAL*, *ITGAM*, and *ITGAX* (Fig EV2B), possibly due to co-translocation with *ITGB2*. Therefore, YAP-induced *ITGB2* should mainly exist as LFA-1, a heterodimer with *ITGAL*. Consistently, expression of active YAP strongly promoted the adhesion of A375 cells to ICAM-1, an LFA-1 ligand, especially in the presence of Mn^{2+} , which increases the affinity of integrins [32] (Fig 2B). In contrast, YAP did not promote the adhesion of A375 cells to VCAM-1, an integrin $\alpha4\beta1$ ligand (Fig 2B). By immunofluorescence, YAP-induced

ITGB2 partially localize to actin-rich lamellipodia but not focal adhesion-like structures when cells were plated on ICAM-1-coated surfaces (Fig EV2C). Thus, YAP promotes cancer cell adhesion to LFA-1 ligand, possibly through the induction of *ITGB2*.

We further generated *ITGB2* knockout A375 cells by CRISPR/Cas9-mediated genome editing using two independent single guide RNAs (sgRNAs) (Fig 2C). The ability of these cells to migrate through transwell inserts was examined. While YAP strongly promoted cell migration toward ICAM-1-coated surfaces, knockout of *ITGB2* largely reduced the effect (Fig 2D and E). Invasion through the endothelium is a major barrier for cancer metastasis [33]. We thus investigated whether YAP-induced *ITGB2* could further facilitate transendothelial invasion. Pretreatment of human umbilical vein endothelial cells (HUVEC) with IL-1 β or TNF- α induced ICAM-1 expression to a similar level (Fig EV2D). Remarkably, YAP strongly induced A375 cells to invade through TNF- α pretreated HUVEC cell layer in a manner largely dependent on *ITGB2* (Fig 2F and G). Furthermore, while YAP promoted inoculated cancer cells to form lung lesions in nude mice, knockout of *ITGB2* blocked the effect (Fig 2H). These data indicate that YAP-induced *ITGB2* expression facilitates cancer cells to extravasate through the endothelium.

PRDM4 is a transcription factor interacting with YAP WW domains

We next investigated how YAP induces *ITGB2* expression. TEAD family transcription factors interact with YAP in a serine 94 (S94)-dependent manner [22]. Mutation of S94 dramatically repressed *ITGB2* induction by YAP (Fig 3A and B). Interestingly, mutation of YAP WW domains also largely abolished *ITGB2* induction (Fig 3A and B). In contrast, the induction of *CTGF* was inhibited by mutation of S94 but not the WW domains (Fig EV3A). However, *ITGB2* expression was not reduced by knockdown of YAP WW domain-interacting transcription factors, such as RUNX (data not shown). Thus, other transcription factors mediating YAP-induced gene expression may exist.

We next investigated YAP-interacting proteins via tandem affinity purification (TAP). Mass spectrometry identified known YAP-interacting PPXY-containing proteins, including LATS1 and AMOTL2 (Fig 3C). Interestingly, we also recovered a potential transcription regulator, PRDM4, which has two PPXY motifs, six zinc finger motifs, and a PR domain (20–30% identical to the SET domain of histone lysine methyltransferase; Fig 3C and D) [34]. By co-immunoprecipitation, we confirmed that YAP specifically interacts with PRDM4 (Fig 3E). Furthermore, although we did not find an antibody suitable for detection of endogenous PRDM4, we confirmed that endogenous YAP could interact with ectopically expressed PRDM4 (Figs 3F and EV3B). In addition, mutation of each WW domain of YAP or PPXY motif of PRDM4 strongly inhibited their interaction (Figs 3F and G, and EV3B and C). Thus, PRDM4 is a transcription factor interacting with YAP WW domains.

Remarkably, PRDM4 has also been recovered through an independent approach. We have previously reported the identification of TEADs as YAP target transcription factors in a luciferase reporter-based screen of a plasmid library encoding Gal4-fusion human transcription factors [22]. Interestingly, PRDM4 turned out to be activated by YAP to a similar level as TEADs in this screen (Fig 3H). Using the same reporter assay, we demonstrated that mutation of either YAP WW domains or PRDM4 PPXY motifs abolished reporter

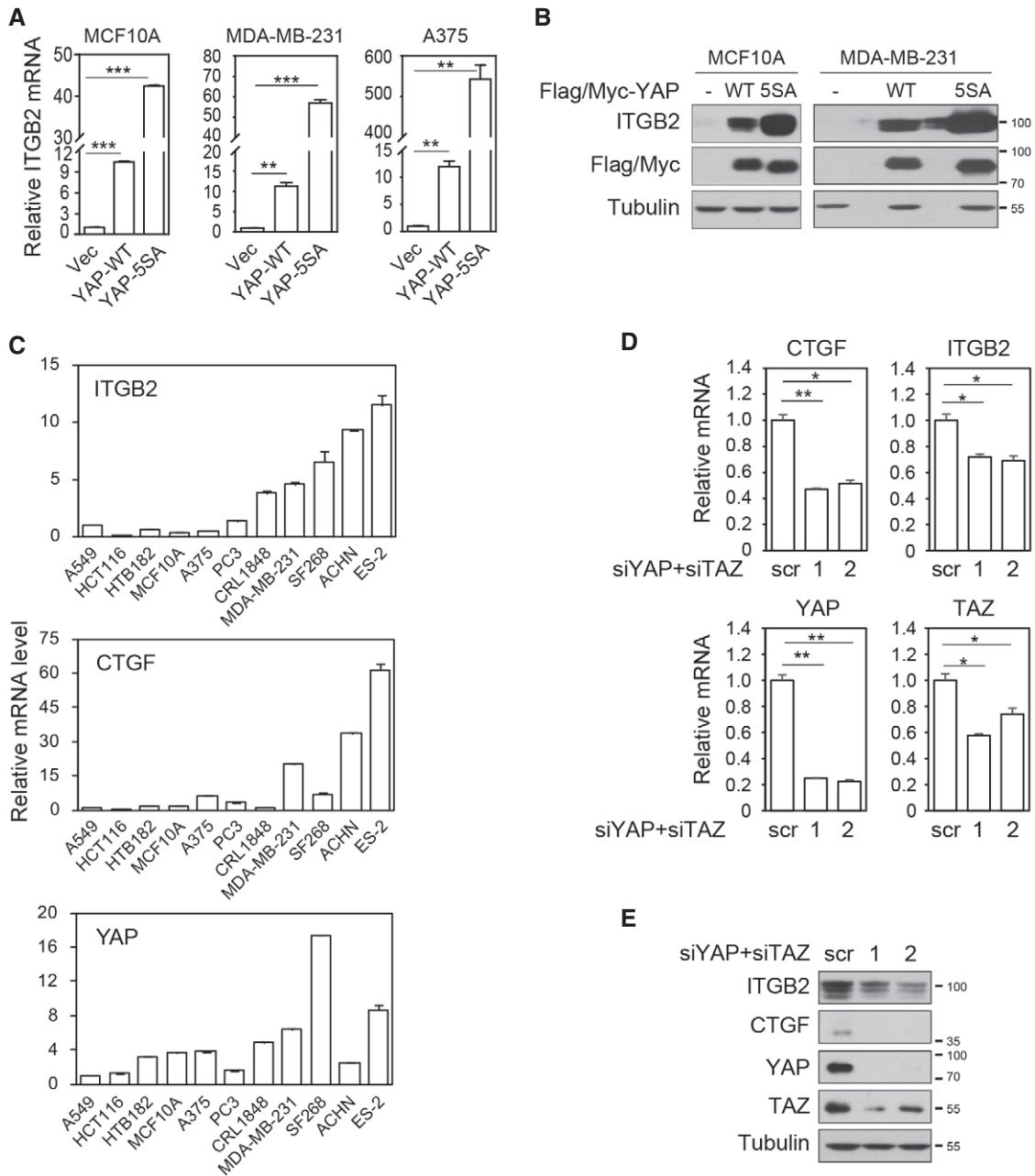


Figure 1. YAP induces ITGB2 expression in cancer cells.

A, B YAP induces ITGB2 expression. mRNA levels were determined by quantitative RT-PCR (qPCR) (A), and protein levels were examined by Western blotting (B). Molecular weight markers in kDa. Empty vector (Vec) was used as control.

C ITGB2 expression correlates with YAP activity in different cell lines. The mRNA levels were determined by qPCR (A549 as unit one).

D, E Endogenous YAP and TAZ regulate ITGB2 expression. ACHN cells were transfected with siRNAs. mRNA levels (D) and protein levels (E) of ITGB2 were determined.

Data information: Results are representatives of three independent experiments. Values represent mean \pm s.d. from three technical repeats. * $P < 0.05$; ** $P < 0.01$; *** $P < 0.001$.

Source data are available online for this figure.

activation by YAP and PRDM4 (Fig 3I and J). In addition, the transcriptional activity of the YAP-PRDM4 complex is inhibited by the Hippo pathway kinases (Fig 3K). Taken together, via two independent unbiased approaches, we identified PRDM4 as a YAP WW domain-interacting transcription factor.

PRDM4 cooperates with TEAD to mediate YAP-induced ITGB2 expression

We next determined whether PRDM4 mediates ITGB2 induction by YAP. Expression of PRDM4 to five times the endogenous level leads to a

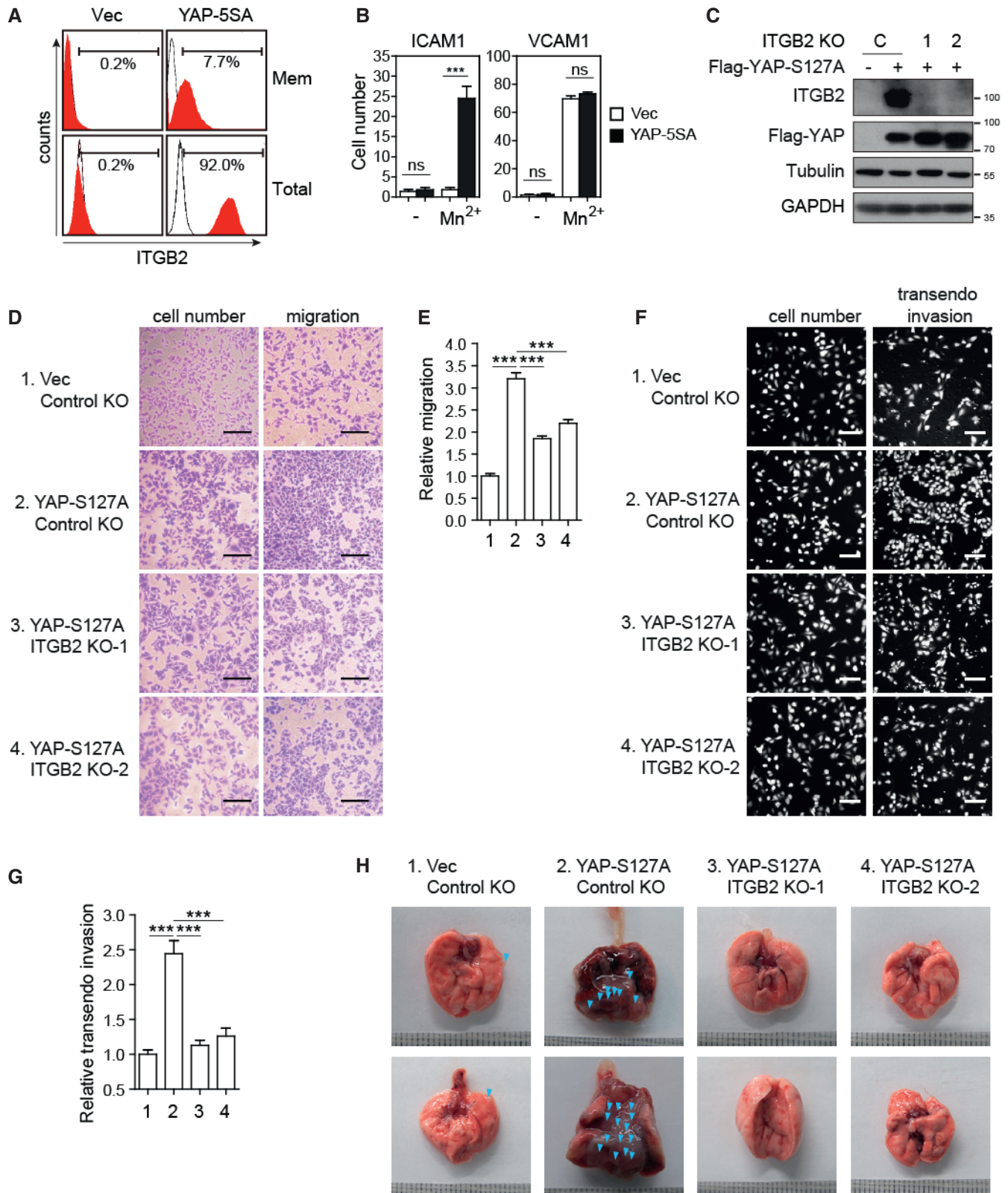


Figure 2.

ninefold induction of *ITGB2*, which was hampered by mutation of PPXY motifs (Fig EV4A). More importantly, knockdown of PRDM4 markedly reduced *ITGB2* expression in ACHN and PC3 cells (Figs 4A and B, and

EV4B). Furthermore, knockdown of TEAD1/3/4 also strongly repressed *ITGB2* expression (Fig 4C and D). Therefore, both PRDM4 and TEAD play important roles in regulation of *ITGB2* expression.

Figure 2. ITGB2 mediates YAP-induced cancer cell transendothelial invasion.

- A YAP-induced *ITGB2* partially localizes to plasma membrane. Flow cytometry analysis of A375 stable cells for total and membrane *ITGB2* expression. Empty vector (Vec) was used as control.
- B YAP promotes cell adhesion to ICAM1-coated surface. A375 stable cells were subjected to flow chamber assay with or without 1 mM Mn^{2+} .
- C Knockout of *ITGB2* in A375 cells expressing active YAP-127A mutant. Lysates were examined by Western blotting.
- D, E *ITGB2* knockout suppresses YAP-induced cell migration. Cells were subjected to transwell migration assay. A parallel set of cells was seeded into regular culture plates as a control for cell number. Relative migration was calculated by normalization of migrated cells with the number of total seeded cells (E).
- F, G *ITGB2* knockout suppresses YAP-induced transendothelial invasion. A375 stable cells were labeled with CFSE and then seeded onto a layer of TNF- α -pretreated HUVEC endothelium formed in transwells. A parallel set of cells was seeded into regular culture plates as a control for cell number. Invasion was quantified in (G).
- H *ITGB2* facilitates YAP-induced cancer cell metastasis *in vivo*. 1.5×10^6 of each stable cell was injected into nude mice via the tail vein. Mice were sacrificed after 30 days. Two representative lungs out of five were presented. Arrowheads indicate tumors.

Data information: Results are representatives of three independent experiments. Values represent mean \pm s.d. from three technical repeats. *** $P < 0.001$. Scale bars 100 μ m. Source data are available online for this figure.

To understand how TEAD and PRDM4 regulate *ITGB2* expression, we constructed a luciferase reporter driven by a 2 kb *ITGB2* promoter (Fig 4E). Co-expression of YAP with either PRDM4 or TEAD2 potently induced the reporter, which was further enhanced by combination of all three proteins (Fig 4F). We further truncated the promoter into two complementary 1 kb reporters, distal and proximal (Fig 4E). While YAP-TEAD activates only the proximal reporter (Fig 4G), YAP-PRDM4 could activate both (Fig 4H). However, chromatin immunoprecipitation (ChIP) of endogenous YAP, TEAD1, or ectopically expressed PRDM4 indicated that they all bind around the -0.5 kb region of the *ITGB2* promoter (Fig 4I). Furthermore, deletion of PRDM4 zinc finger motifs, which mediate DNA-binding, abolished cooperation with YAP to activate *ITGB2* reporter (Fig EV4C). The PR domain of PRDM4 is catalytically inactive [35]. Indeed, even when we further mutated Y528, a residue conserved in the active site of PRDM9, and G444, a residue important for PR domain structure [35], it still cooperated with YAP to activate the *ITGB2* reporter (Fig EV4D). The proximal 1 kb promoter of *ITGB2* contains three perfect TEAD binding sites and a stretch of eight GGCATC repeats that also fit TEAD binding consensus (Fig 4E), as well as two GAAAC motifs that match the core sequence of a PRDM4 binding consensus (Fig 4E). However, mutation of sites other than the GGCATC repeats did not affect reporter activation by YAP, TEAD, or PRDM4 (Fig EV4E and F). Nevertheless, deletion of the GGCATC repeats largely eliminated induction by YAP/TEAD (Fig EV4G), suggesting their functional importance. The exact PRDM4 binding sites remains elusive. While mouse *ITGB2* could not be induced by YAP, its promoter contains potential TEAD and PRDM4 binding sites, and could be strongly transactivated (Fig EV4H). Therefore, the inability of mouse *ITGB2* to respond to YAP is possibly due to lack of other conditions such as additional transcription factor or chromatin condition. Since YAP interacts with TEAD and PRDM4 through distinct domains, we examined the possibility of a heterotrimeric complex. Indeed, when YAP, TEAD4, and PRDM4 were co-expressed, immunoprecipitation of any of them would pull down the other two (Fig 4J). However, when YAP was omitted, the interaction between TEAD4 and PRDM4 was much weaker (Fig 4J). Taken together, YAP could concomitantly interact with both PRDM4 and TEAD within a proximal region of *ITGB2* promoter to induce its expression.

PRDM4 mediates YAP-induced cell invasion

To further determine the functions of PRDM4, we knocked out this gene in A375 cells, which was confirmed by genomic DNA

sequencing (Fig EV5A). YAP-induced *ITGB2* expression was largely suppressed in these cells (Fig 5A and B). The incompleteness of this suppression suggests a basal activity of YAP to induce *ITGB2* expression without PRDM4, likely via TEAD. Importantly, knockout of PRDM4 largely blocked the transactivation of *ITGB2* reporter by YAP (Fig EV5B), indicating a critical role of PRDM4 in the interaction of YAP with *ITGB2* promoter. Furthermore, we observed that knockout of PRDM4 clearly inhibited YAP-expressing A375 cells to invade the endothelium (Fig 5C and D). Taken together, PRDM4 is a transcription factor partner of YAP mediating YAP-induced cell invasion.

Deregulation of *ITGB2* and *PRDM4* expression in metastatic prostate cancer

We have demonstrated that LATS1/2 were specifically down-regulated in metastatic prostate cancer, thus may contribute to metastasis due to YAP activation [25]. Therefore, we investigated the expression of *ITGB2* and *PRDM4* in prostate cancer clinical samples. We compiled RNA-seq data from the Cancer Genome Atlas (TCGA) dataset [36], which contains only normal and localized prostate cancer, with several datasets of the database of Genotypes and Phenotypes (dbGaP) containing late-stage prostate cancer specimens [37–40]. This led to a total of 87 cases of normal prostate tissue, 577 cases of localized prostate cancer, and 147 cases of metastatic prostate cancer. Interestingly, the mRNA levels of *ITGB2* and *PRDM4* are significantly higher in metastatic prostate cancer when compared to normal tissue or clinically localized cancer (Fig 5E). Although the mRNA level of YAP is lower in metastatic cancer samples (Fig 5E), YAP activity is higher as indicated by the activation of a YAP-induced gene signature [41] (Fig EV5C), likely due to deregulated Hippo pathway activity. Furthermore, there is a significant correlation between *ITGB2* and *PRDM4* expression in prostate cancer samples (Fig 5F). These data suggest that activation of YAP and PRDM4 may contribute to the elevated *ITGB2* expression in metastatic prostate cancer.

PRDM4 contributes to YAP-induced tumorigenesis

We further examined whether PRDM4 also plays a role in YAP-induced tumorigenesis. Expression of active YAP clearly promoted tumorigenesis of A375 cells in nude mice as xenografts. However, this effect was abolished by *PRDM4* knockout (Figs 5G and EV5D).

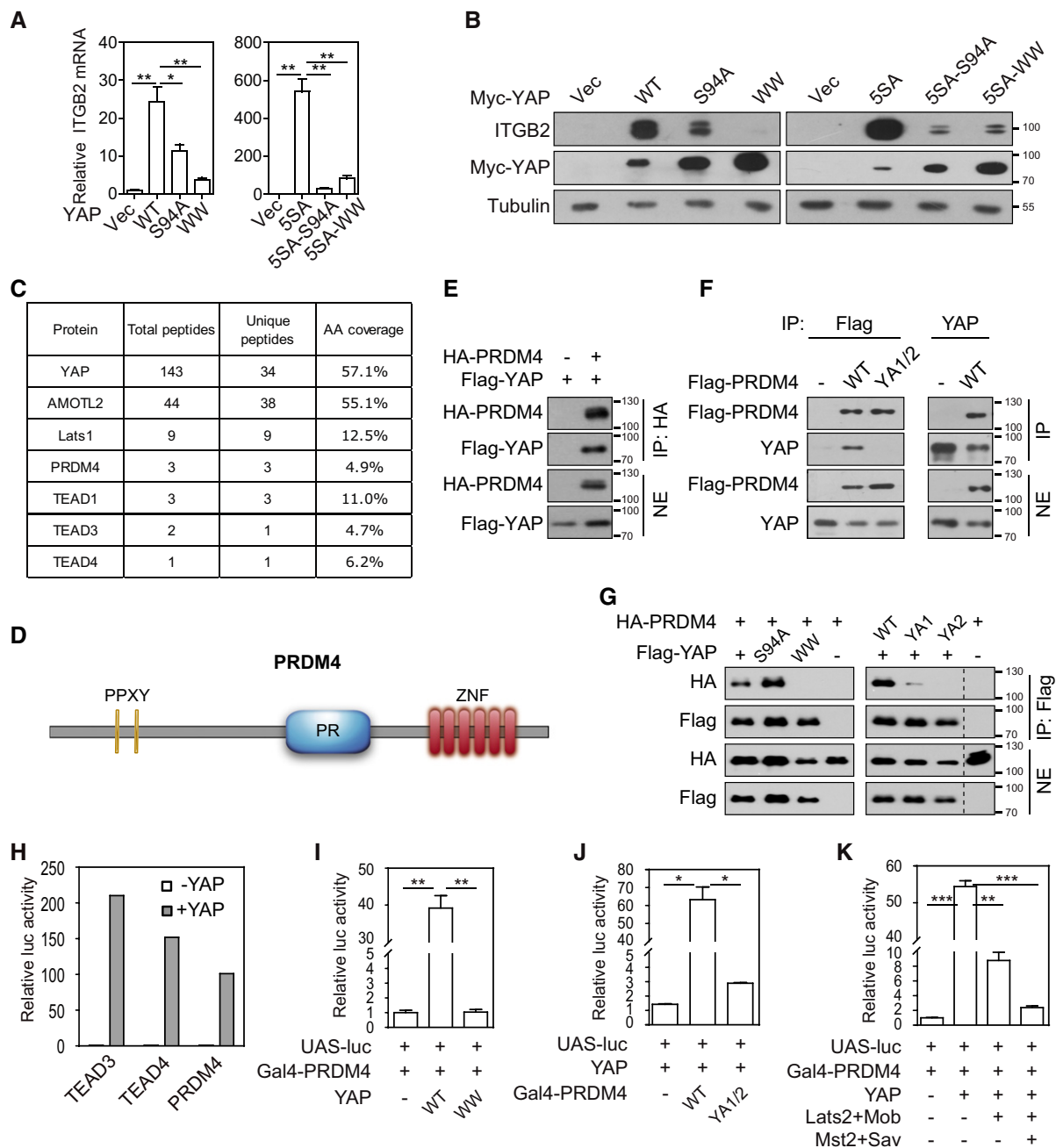


Figure 3. Identification of PRDM4 as a transcription factor interacting with YAP WW domains.

A, B YAP induces *ITGB2* expression in a TEAD- and WW domain-dependent manner. *ITGB2* mRNA (A) and protein (B) levels in MCF10A stable cells were determined. Empty vector (Vec) was used as control.

C TAP-mass spectrometry identified PRDM4 as a YAP-interacting protein. The number of peptide hits for PRDM4 and several known YAP-interacting proteins is shown.

D Illustration of PRDM4 domain organization. ZNF, zinc finger motif.

E–G YAP co-immunoprecipitates with PRDM4. Nuclear extracts (NE) were made from transfected HEK293 cells and then immunoprecipitated with indicated antibodies. Samples were examined by Western blotting.

H YAP activated PRDM4 in a transcription factor library screen. The screen was done as described in Materials and Methods. Fold activation of TEAD3, TEAD4, and PRDM4 by YAP are shown.

I–K The WW domains of YAP (I), and the PPXY motifs of PRDM4 (J) are required for the activation of PRDM4, which is inhibited by the Hippo pathway (K). The reporter assay is similar to that in (H).

Data information: Results are representatives of three independent experiments. Values represent mean \pm s.d. from three technical repeats. * $P < 0.05$; ** $P < 0.01$; *** $P < 0.001$.

Source data are available online for this figure.

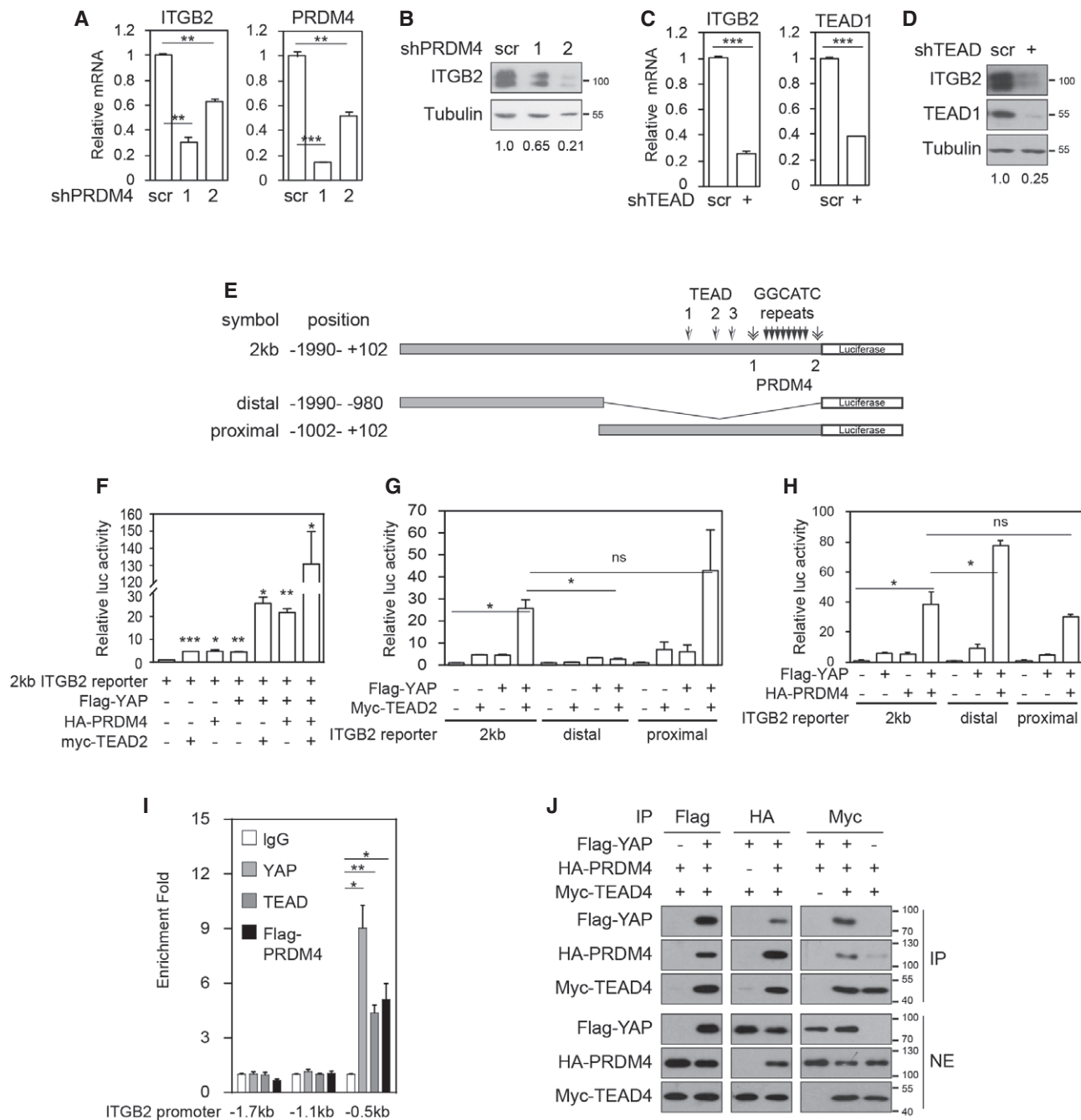


Figure 4. PRDM4 cooperates with TEAD to mediate YAP-induced *ITGB2* expression.

A, B Knockdown of *PRDM4* inhibits *ITGB2* expression. *ITGB2* mRNA (A) and protein (B) levels in shRNA-infected ACHN cells were determined. Relative protein levels of *ITGB2* were quantified.

C, D Knockdown of *TEAD* inhibits *ITGB2* expression. ACHN cells infected with scramble or shRNA targeting *TEAD1/3/4*.

E Illustration of *ITGB2* reporters in scale. Potential TEAD and PRDM4 binding sites as well as a GGCATC repeats were indicated.

F YAP, PRDM4, and TEAD2 coordinately activate *ITGB2* reporter. HEK293T cells were transfected and luciferase activity was normalized to co-transfected β -galactosidase activity. Indicated *P*-values are in comparison with the reporter only sample.

G, H YAP-TEAD2 activates the proximal promoter, and YAP-PRDM4 activates both the distal and proximal promoters of *ITGB2*. Experiments were similar to these in (F).

I YAP, TEAD, and PRDM4 bind to a proximal 0.5 kb region of *ITGB2* promoter. Control or Flag-PRDM4-expressing HepG2 cells were processed for ChIP followed by qPCR detection.

J YAP, TEAD, and PRDM4 could form a heterotrimeric complex. NE of transfected HEK293T cells were immunoprecipitated with indicated antibodies.

Data information: Results are representatives of three independent experiments. Values represent mean \pm s.d. from three technical repeats. **P* < 0.05; ***P* < 0.01; ****P* < 0.001.

Source data are available online for this figure.

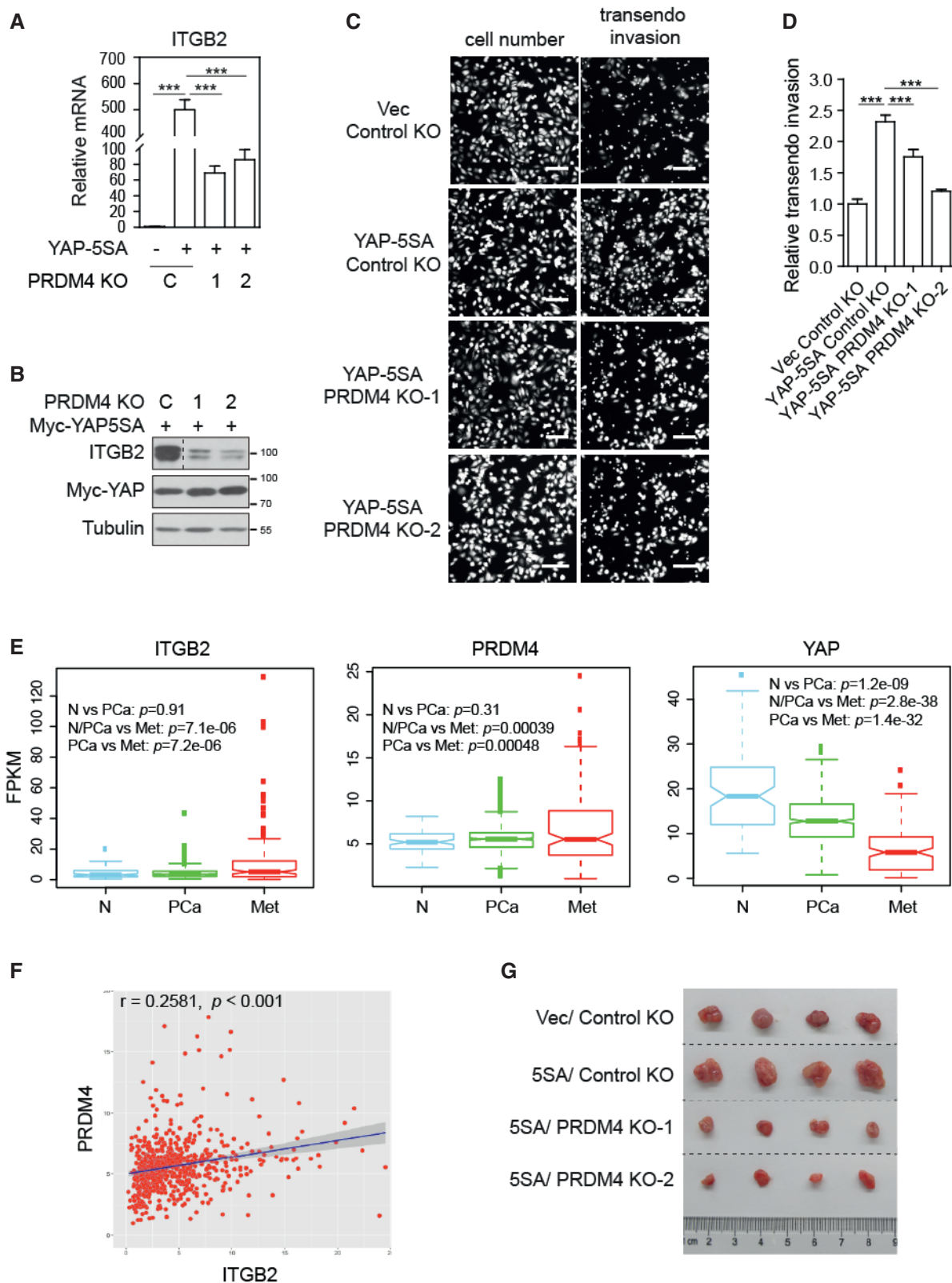


Figure 5.

Nevertheless, the knockout of *ITGB2* did not consistently affect YAP-induced proliferation and tumorigenesis (data not shown). Therefore, YAP-PRDM4 promotes tumorigenesis likely through

other target genes. We thus compared genes regulated by YAP and PRDM4 in profiling datasets. PRDM4-regulated genes have been studied in PRDM4 knockout murine embryonic stem (ES) cells [42].

Figure 5. PRDM4 mediates YAP-induced cell invasion and deregulation of *ITGB2* and *PRDM4* expression in metastatic prostate cancer.

- A, B Knockout of *PRDM4* inhibits *ITGB2* induction by YAP. *ITGB2* mRNA (A), and protein (B) levels were determined.
- C, D Knockout of *PRDM4* inhibits YAP-induced transendothelial migration. Experiments were similar to these in Fig 2F. Scale bars 100 μ m. Invasion was quantified in (D).
- E The mRNA levels of *ITGB2* and *PRDM4* are significantly increased in metastatic prostate cancer. N, normal; PCa, localized prostate cancer; Met, metastatic prostate cancer. The boxes are 25th to 75th percentiles, and the whiskers are minimum and maximum values. Points beyond the whiskers are outliers.
- F Correlation of *PRDM4* and *ITGB2* mRNA levels in prostate cancer. FPKM values of *PRDM4* and *ITGB2* in prostate cancer samples were extracted from the TCGA and the dbGaP databases, and their correlation was determined by R ggplot2 package.
- G *PRDM4* plays an important role in YAP-induced tumorigenesis. A375 stable cells were injected subcutaneously into nude mice. Tumors were dissected after 17 days.
- Data information: Results are representatives of three independent experiments. Values represent mean \pm s.d. from three technical repeats. ****P* < 0.001. Source data are available online for this figure.

Due to the lack of a comparable dataset for YAP, we compared it with YAP-regulated genes in murine liver, as well as human MCF10A and MDA-MB-231 cell lines [22,16,41]. This analysis revealed overlap of genes regulated by PRDM4 and genes regulated by YAP/TAZ (Fig EV5E). Interestingly, gene ontology analysis indicated an enrichment of genes involved in biological processes such as mitosis, cell cycle, DNA replication, cell differentiation, and liver regeneration (Appendix Table S1). The above results indicate that PRDM4 contributes to YAP-induced tumorigenesis possibly by mediating other YAP target gene expression.

In this study, we demonstrate that YAP promotes cancer cell invasion of the endothelium by transcriptional activation of *ITGB2*. Interestingly, it has been reported that primary tumors could induce expression of chemokines in distant tissues that results in recruitment of myeloid cells expressing MAC-1 (an integrin composed of *ITGAM* and *ITGB2*) [43]. Recruited myeloid cells secrete inflammatory factors that further prepare a microenvironment facilitating metastatic lesion [44]. It is therefore intriguing to speculate that YAP-induced *ITGB2* expression could promote adhesion of cancer cells to these inflammatory pre-metastatic niches, and promote the ensuing extravasation.

The WW domains of YAP/Yki mediate interaction with specific proteins, including regulatory proteins such as LATS1/2 and the AMOT family proteins [7,45,46]; DNA-binding transcription factors, such as Smad1, RUNX1/2, p73, Oct4, KLF5, and ErbB4 cytoplasmic domain [47–52,53]; and cofactors, such as WBP2 and NcoA6 (for Yki) [54–56]. NcoA6 is especially interesting because it plays a critical role in the expression of *bona fide* Yki target genes [55,56]. However, in mammals, most YAP target genes depend only on TEAD but not the WW domains. Intriguingly, the YAP transcription activation domain is absent in Yki, suggesting a transfer of the transactivation function away from the WW domains during evolution. Nevertheless, functional studies support that the WW domains of YAP play a role in growth control and oncogenic transformation [28,57]. Here, we demonstrated that by binding to the WW domains, PRDM4 plays a specific role in YAP-induced cell invasion of endothelium through the induction of *ITGB2*. Furthermore, PRDM4 also contributes to YAP-induced tumorigenesis. This study thus demonstrates a PRDM4-mediated transcriptional mechanism of the Hippo pathway in cancer cell invasion and tumor growth.

Most PRDM family proteins, including PRDM4, are catalytically inactive. However, PRDM4 may regulate histone arginine methylation through recruiting protein arginine methyltransferase 5 (PRMT5) [58]. In this report, we found that PRDM4 plays an important role in the induction of *ITGB2* expression possibly by recruiting other cofactors or by modulating the chromatin conformation.

While both YAP and PRDM4 promote embryonic stem cell proliferation and inhibit their differentiation [42,59,60], *Prdm4* knockout mice develop normally without overt abnormalities [42,61]. Thus, PRDM4 likely plays redundant roles with other transcription factors in embryonic development. Nevertheless, it remains possible that PRDM4 plays a specific role in cancer. It was reported that high expression of PRDM4 strongly correlates with gastric cancer recurrence and worse prognosis [62]. Furthermore, in the database of a pathology atlas of the human cancer transcriptome with clinical outcome, the expression of *PRDM4* associates unfavorably with patient survival in liver cancer and melanoma [63]. This is in consistent with that YAP-PRDM4 promotes cancer cell invasion and tumor growth. The structure of YAP WW domains in association with a PPXY-containing ligand has been solved and designing of specific inhibitors targeting interactions mediated by YAP WW domains is therefore possible [64]. Our findings thus suggest the YAP-PRDM4 complex could be a potential target for therapeutic intervention.

Materials and Methods

Antibodies, plasmids, and other materials

Anti-YAP (sc-101199), anti-*ITGB2* (sc-51652) [65], anti-*ITGAM* (sc-1186), and anti-*ITGAX* (sc-1185) antibodies were obtained from Santa Cruz Biotechnology. Anti-*ITGAL* (MA11A10) was obtained from Thermo Fisher. Anti-TEAD1 antibody (610923) was obtained from BD Bioscience. Anti-Flag (F3165), anti- α -tubulin (T5168), and anti-GAPDH (G8795) antibodies were obtained from Sigma. Anti-Myc (MMS-150P-200) and anti-HA (MMS-101R) antibodies were obtained from Covance.

pQCXIH-YAP wild type, S94A, W1 (W199/P202A), W2 (W258/P261A), WW (W199/P202/W258/P261A), 5SA, 5SA-S94A and 5SA-WW plasmids, pCMV-Flag-YAP wild type, S94A, WW plasmids, pcDNA3-HA-MST2, pcDNA3-HA-SAV, pcDNA3-HA-LATS2, pcDNA3-HA-MOB, pRK5-Myc-TEAD4, pRK5-Myc-TEAD2, and 5 \times UAS-luciferase reporter were described before [3,22]. YAP wild type, 5SA, S127A, and S127A-WW were sub-cloned into pLVX-Flag lentiviral vector. PRDM4 was cloned from HeLa cDNA library into pcDNA-HA vector. PRDM4 mutants YA1 (Y97A), YA2 (Y124A), and YA1/2 (Y97/124A) were generated by QuikChange II XL Site-Directed Mutagenesis Kit (Agilent). PRDM4 wild type and mutants were then sub-cloned into pPGS-CITE-neo-HA vector and pLVX-CMV-Flag vector. *ITGB2* 2 kb promoter was cloned from HeLa cell genomic DNA into pGL4.21-TATA vector. The proximal and distal 1 kb *ITGB2* reporter was then made by sub-cloning from the 2 kb

promoter. Mouse *Itgb2* promoter was cloned from NIH-3T3 cell genomic DNA into the pGL4.21-TATA vector.

Human recombinant fibronectin (F4759), TNF- α (T0157) and IL-1 β (SRP3083) were purchased from Sigma. Human ICAM-1 (10346-H03H) and human VCAM-1/CD106 protein (Fc Tag) (10113-H02H-100) were purchased from Sino Biological. Iodoacetamide (IB0359) was purchased from Sangon Biotech. Common chemicals were from Sigma or Sangon Biotech.

Cell culture

HMLE, ACHN, PC3, A549, HTB182, CRL1848, SF268, HCT116, A375, MDA-MB-231, 3T3L1, B16, HUVEC, HEK293, and HEK293T cells were gift from Dr. Kun-Liang Guan's laboratory at the year 2012. MCF10A cells were purchased (year 2009) from ATCC, where they were characterized by DNA finger printing. Cell line authentication was not done in the laboratory. MCF10A and HMLE cells were cultured in DMEM/F12 medium (Life Technologies) supplemented with 5% horse serum (Life Technologies), 20 ng/ml EGF, 0.5 μ g/ml hydrocortisone, 10 μ g/ml insulin, 100 ng/ml cholera toxin, and 50 μ g/ml penicillin/streptomycin (P/S). ACHN, PC3, A549, HTB182, CRL1848, and SF268 cells were cultured in RPMI1640 medium (Life Technologies) supplemented with 10% FBS (Life Technologies) and 50 μ g/ml P/S. HCT116, A375, MDA-MB-231, 3T3L1, B16, HEK293, and HEK293T cell were cultured in DMEM medium (Invitrogen) supplemented with 10% FBS and 50 μ g/ml P/S. ES-2 cells were gift from Dr. Hengyu Fan's laboratory and were cultured in McCoy's 5a medium supplemented with 10% FBS and 50 μ g/ml P/S. HUVEC cells were cultured in EGM-2 medium (Lonza) supplemented with 50 μ g/ml P/S. BMSSC cells were isolated from femurs and tibias of 7–10 weeks healthy ICR mice (male) by opening bone cavity and flushing out marrow, followed by culture in alpha-MEM medium (Life Technologies) with 10% FBS, 1 \times glutamax (Life Technologies) and 50 μ g/ml P/S. Mycoplasma test for cell culture was done in a yearly basis using MycoPlasma Detection Kit (biotool.com). Cells used in experiments were within 10 passages from thawing.

Transfection and viral infection

Transfection of plasmids was performed using Lipofectamine (Life Technologies) according to the manufacturer's instructions. Transfection of siRNAs was performed using Lipofectamine RNAiMAX (Life Technologies) according to the manufacturer's instructions.

To generate stable cells, lentiviral or retroviral infections were used. Briefly, HEK293T cells were co-transfected with viral plasmids and packaging plasmids. Forty-eight hours after transfection, culture medium was supplemented with 5 μ g/ml polybrene, filtered through a 0.45 μ m filter, and used to infect cells of interest. Thirty-six hours after infection, cells were selected with respective antibiotics in culture medium.

RNA interference

siRNAs against human or mouse YAP and TAZ were synthesized by Ribobio:

| | |
|----------------|---------------------|
| siRNA h/mYAP#1 | CCACCAAGCTAGATAAAGA |
| siRNA hYAP#2 | GGTCAGAGATACTTCTTAA |
| siRNA h/mYAP#3 | GCACCTATCACTCTCGAGA |
| siRNA hTAZ#1 | CCAAATCTCGTGATGAATC |
| siRNA hTAZ#2 | CCGCGAGGCTCATGAGTAT |
| siRNA mTAZ#1 | GATGAATCCGTCCTCGGTG |
| siRNA mTAZ#2 | TCATTCCGAGATCCGGCTG |

shRNAs against YAP and TEAD1/3/4 have been previously reported [22]. To generate shRNAs against PRDM4, oligonucleotides were cloned into pLKO.1 with the AgeI/EcoRI sites. Oligonucleotide sequences are listed as below:

| | |
|---------------------------|---|
| shRNA hPRDM4 #1-sense | CCGGGTAGGACATGGTGGTGTGATACTCGAGTATCACACCACCATGTCCTACTTTTTTC |
| shRNA hPRDM4 #1-antisense | AATTGAAAAAGTAGGACATGGTGGTGTGATACTCGAGTATCACACCACCATGTCCTAC |
| shRNA hPRDM4 #2-sense | CCGGAAGGAAGGAAGGAATAATCCTCGAGGATTATTCCTTCCTCCCTTTTTTTC |
| shRNA hPRDM4 #2-antisense | AATTGAAAAAGGAAGGAAGGAATAATCCTCGAGGATTATTCCTTCCTCCCTTCCT |

CRISPR-Cas9 mediated knockout

CRISPR-Cas9 technology was used to generate ITGB2 and PRDM4 knockout cells. Two independent sgRNAs were designed by the Zhang laboratory CRISPR Design Tool. Annealed oligonucleotides were ligated into the PEP-KO vector digested with SapI. For knockout, plasmids were transfected into A375 cells. Forty-eight hours later, cells were selected with 2 μ g/ml puromycin for another 48 h. Live cells were collected and re-plated at low density for colony formation. Individual clones were examined by Western blotting or genomic DNA sequencing. sgRNA hairpin sequences are listed as below:

| | |
|----------------|----------------------|
| sgRNA hITGB2#1 | GGGCTGCTCCCTCGGGTG |
| sgRNA hITGB2#2 | CCCGGAATGCATCGAGTCG |
| sgRNA hPRDM4#1 | TGAAATGAACCTGAGTCCAG |
| sgRNA hPRDM4#2 | AGCAATGCCTGCCAGTCTC |

Luciferase assays

For luciferase reporter assays, HEK293-T cells were seeded in 12-well plates. Cells were then transfected with the reporter, CMV- β -gal, and indicated plasmids. 36 h after transfection, cells were lysed and luciferase activity was assayed using the Luciferase Assay System (Promega) following the manufacturer's instructions. All luciferase activities were normalized to β -galactosidase activity.

The Gal4-TF library screen has been previously reported [22]. Briefly, luciferase assay was carried out as stated above in 96-well

format and the reading from the well with YAP was divided by the reading of the respective well without YAP to get the activation fold. The screen was done in duplicate.

Western blotting

Western blotting was performed using standard protocol. Briefly, cells were lysed with 1% SDS lysis buffer and protein concentration was determined using the BCA Assay Kit (Pierce). Protein samples were resolved on SDS-PAGE and then transferred to PVDF membranes. Membranes were blocked with 5% skimmed milk, incubated sequentially with primary and secondary antibodies, and then washed. Protein expression was detected by ECL Detection Reagent (Pierce).

The expression of ITGB2 protein was determined by Western blotting after resolving on non-reducing gels. Cells were washed once with cold PBS, lysed with cold lysis buffer (20 mM Tris pH 7.5, 100 mM NaCl, 0.5 mM PMSF, 5 mM iodoacetamide, 50 mM NaF, 1 mM Na₃VO₄, 10 mM EDTA, 10% glycerol, and 1% NP-40), and then incubated on ice for 30 min. Cell lysates were centrifuged at 15,924 *g* at 4°C for 15 min. Supernatants were boiled at 65°C for 5 min. Lysates were mixed with 2× SDS loading buffer (0.125M Tris PH 6.8, 4% SDS, 20% glycerol, 0.002% bromophenol blue). Samples were then processed for Western blotting as usual.

RNA isolation and real-time PCR

Total RNA was isolated from cells using Trizol reagent (Life Technologies). cDNA was synthesized by reverse transcription using PrimeScrip RT Master Mix (Takara) and subjected to real-time PCR with gene-specific primers in the presence of SYBR Green (Applied Biosystems). Relative abundance of mRNA was calculated by normalization to hypoxanthine phosphoribosyltransferase 1 (HPRT) mRNA.

Nuclear extraction and immunoprecipitation

To detect YAP-PRDM4 interaction, nuclear extracts (NE) were made from respective cells and then processed for immunoprecipitation. Cells were washed once with PBS and once with low salt buffer (10 mM HEPES pH 7.9, 10 mM KCl, 0.1 mM EDTA, 0.1 mM EGTA). Cells were then scraped down in low salt buffer with additive (protease inhibitor cocktail, 1 mM DTT, 0.5 mM PMSF, 2.5 mM NaF) and incubated on ice for 5 min. Samples were then passed through 25G needle for 10 times and centrifuged at 1,000 *g* at 4°C for 15 min. Pellets were then incubated with high salt buffer (20 mM HEPES pH 7.9, 0.4 M NaCl, 1 mM EDTA, 1 mM EGTA, 1 mM DTT, 1 mM PMSF, 1% NP40) on ice for 1 h. Samples were then centrifuged at 20,000 *g* at 4°C for 10 min, and supernatants were taken as nuclear extracts. Nuclear extracts were diluted four times with dilution buffer (10 mM HEPES pH 7.4, 50 mM NaF, 1 mM EDTA, protease inhibitor cocktail, 1% NP40) and then used for immunoprecipitation. For immunoprecipitation, nuclear extracts were incubated with respective antibodies at 4°C overnight. Protein G or protein A Sepharose (GE Healthcare) was then added and further incubated at 4°C for 2 h. The resins were then washed three times and boiled in SDS sample buffer before analysis by Western blotting.

Chromatin immunoprecipitation

ChIP assays were performed using an EZ-ChIP kit from Millipore according to the manufacturer's instructions. Briefly, cells were cross-linked, lysed, and sonicated to generate DNA fragments with an average size of 0.5 kb. ChIP was performed using 5 μg control IgG or antibodies against YAP, TEAD1, or Flag. The immunoprecipitates were then washed and eluted. The eluates were then de-cross-linked, and DNA was purified for PCR analysis. PCR primers for ChIP assay:

| | |
|-------------------------|------------------------|
| ITGB2-chip-1F (−1.7 kb) | TTCCTCACTCAGCAGCCT |
| ITGB2-chip-1R | TCAGTTCTG AAGGCACCT |
| ITGB2-chip-2F (−1.1 kb) | ACCATTCCACGTGCCTGT |
| ITGB2-chip-2R | GAATGAGTAT GACTGTGTT C |
| ITGB2-chip-3F (−0.5 kb) | TTCAGGATGGAAATGCCGTG |
| ITGB2-chip-3R | ATGGGGGCTT CCTAAGCTCA |

Cell migration assay

Cell migration assay was performed using BD Falcon Cell culture inserts for 24-well plates with 8.0 μm pore size. Bottom sides of inserts were pre-coated with 4 μg/ml ICAM1 protein. A375 stable cells were cultured in serum-free medium for 12 h before use. 200 μl 2.5 × 10⁵ cells/ml cell suspensions in serum-free medium was seeded into the inserts, and 800 μl 10% FBS-containing medium was added into the lower chambers. Cells were cultured for 10 h, and the inserts were then stained with 0.5% crystal violet. Cells on the upper side of the inserts were wiped off, and the bottom sides of the inserts were pictured.

Transendothelial cell invasion

2.5 × 10⁴ HUVEC cells were cultured for 36 h in the upper chamber of transwell inserts and then treated with 10 ng/ml TNF-α for 12 h. 5 × 10⁴ A375 stable cells were labeled with 5 μM CFSE (Life Technologies) and seeded into transwell filters on top of the HUVEC monolayers in serum-free medium. 10% FBS-containing medium was added into lower chambers. Cells were cultured for 10 h, and cells invaded to the bottom side of the inserts were imaged by fluorescence microscopy.

Flow chamber cell adhesion assay

The flow chamber assay was performed as described before [66]. A polystyrene petri dish to be used as the lower wall of the chamber was coated with a 5 mm diameter, 20 μg/ml purified human ICAM-1 Fc or VCAM1 Fc in coating buffer (PBS, 10 mM NaHCO₃, pH 9.0) for 1 h at 37°C, then blocked by 2% human serum albumin in coating buffer for 1 h at 37°C. EDTA-pretreated cells were diluted to 1 × 10⁶/ml in Ca²⁺- and Mg²⁺-free Hank's balanced salt solution with 10 mM HEPES and 0.5% BSA with or without Mn²⁺ and then infused in the flow chamber. Cells were allowed to accumulate for 30 s at 0.3 dyne/cm² and for 10 s at 0.4 dyne/cm². Then, shear stress was increased every 10 s from 1 dyne/cm² up to 32 dyne/cm² in 2-fold increments. The number of cells

remaining bound at the end of each 10-s interval for 5 min was recorded by microscope.

Flow cytometry

To detect the level of plasma membrane-localized ITGB2, cells were dissociated by cell dissociation buffer (Thermo Fisher), washed once with cold PBS, and resuspended in PBS containing 5% FBS. Cells were then counted, and 2×10^5 cells were incubated in 200 μ l 5% FBS/PBS containing anti-ITGB2 antibody (Santa Cruz sc-51652) at 4°C for 1 h. Cells were then washed three times with cold PBS and incubated with PE-conjugated anti-mouse IgG secondary antibody (Miltenyi Biotec) at 4°C for 1 h. Cells were then washed three times with cold PBS and resuspended in 500 μ l PBS for analysis on Beckman FC 500 MCL. Data were analyzed using FlowJo software. For detection of total ITGB2, cells were fixed with 2% PFA/PBS and permeabilized with 0.2% Tween-20/PBS. 0.2% Tween-20 was also added during the primary antibody incubation step and the following wash step.

Tandem affinity purification

Tandem affinity purification of YAP has been previously reported [45]. Briefly, MCF10A stable cells were lysed with buffer containing 0.3% CHAPS. Lysates were first incubated with anti-Flag-antibody-conjugated resin for 2 h at 4°C and washed three times with lysis buffer. Bound proteins were then eluted with elution buffer containing 200 ng/ μ l 3 \times Flag peptide. The eluates were further incubated with streptavidin-conjugated resin for 2 h at 4°C. Resins were washed and then eluted with buffer containing 4 mM biotin. Samples were then processed for MS/MS analysis.

Prostate cancer gene expression data analysis

Prostate cancer RNA-seq data from TCGA were downloaded from the Genomic Data Commons [67]. RNA-seq data of late-stage prostate cancer with accession numbers phs000443 [37,38], phs000915 [39], and phs000909 [40] were downloaded from dbGaP. All data were normalized to fragments per kilobase of transcript per million mapped reads (FPKM). Boxplots and correlation plots were generated in R.

Xenograft tumorigenesis model

All animal study protocols were approved by the Zhejiang University Animal Care and Use Committee. Nude mice (nu/nu, male 6- to 8-week-old) were purchased from Shanghai SLAC Laboratory Animal Company and were housed in SPF grade facility. They were injected subcutaneously into the two flanks with 5×10^5 A375 stable cells. After 17 days, tumors were dissected, weighed, and photographed. For lung metastasis assay, 1.5×10^6 of indicated stable A375 cells was injected in 200 μ l PBS via lateral tail vein. After 30 days, lungs were dissected and pictured.

PRDM4- and YAP-regulated genes analysis

To determine genes potentially co-regulated by PRDM4 and YAP, we compared PRDM4- and YAP-regulated gene datasets. Datasets of

PRDM4-dependent genes in murine embryonic stem cells, YAP-induced genes in MCF10A cell line, and YAP/TAZ-dependent genes in MDA-MB-231 cell line were from NCBI Gene Expression Omnibus Database (accession numbers GSE46308, GSE13218, and GSE59230, respectively). Datasets were analyzed with GEO2R (<https://www.ncbi.nlm.nih.gov/geo/info/geo2r.html>). For PRDM4-dependent genes in murine embryonic stem cells and YAP/TAZ-dependent genes in MDA-MB-231 cell line, genes with adjusted *P*-value < 0.01 and logFoldChange < -0.4 were considered significant. For YAP-induced genes in MCF10A cell line, genes with adjusted *P*-value < 0.01 and logFoldChange > 1 were considered significant. Dataset of YAP-induced genes in murine liver is from published paper [16]. Enriched gene ontology biological process terms of overlap gene lists were analyzed by Gene Ontology Consortium (<http://geneontology.org/>) with *P*-value < 0.05.

Statistical analysis

The *P*-values were determined by Student's *t*-tests.

Expanded View for this article is available online.

Acknowledgements

We thank Dr. Kun-Liang Guan for critical reagents; Dr. Hongbin Ji for HTB182 and CRL1848 cell lines; Dr. Hengyu Fan for ES-2 cell line; and Dr. Zongping Xia for PEP-KO and pGL4.21-TATA vectors. The results are in part based upon data generated by the TCGA Research Network: <http://cancer.gov/nome.nih.gov/>. The dbGaP project provided access to the datasets (accession nos: phs000443, phs000915, and phs000909). This work was supported by grants to B. Zhao from the National Key R&D Program of China (2017YFA0504502), the National Natural Science Foundation of China General Project (31471316), Key Project (81730069), and International Collaboration Project (31661130150), the 111 project (B13026), the Fundamental Research Funds for the Central Universities, the Qianjiang Scholar Plan of Hangzhou, the Thousand Young Talents Plan of China, and the Newton Advanced Fellowship from the Academy of Medical Sciences, UK.

Author contributions

BZ and HL conceived the project. BZ, HL, and XD designed the study. HL, XD, XC, HY, XJ, HZ, SS, YS, and HZ performed experiments. BZ, HL, XD, JCZ, and JY analyzed data. JC, LL, and X-HF provided conceptual advices. BZ and HL wrote the manuscript with comments from all authors.

Conflict of interest

The authors declare that they have no conflict of interest.

References

- Pan D (2010) The hippo signaling pathway in development and cancer. *Dev Cell* 19: 491–505
- Yu FX, Zhao B, Guan KL (2015) Hippo pathway in organ size control, tissue homeostasis, and cancer. *Cell* 163: 811–828
- Zhao B, Wei X, Li W, Udan RS, Yang Q, Kim J, Xie J, Ikenoue T, Yu J, Li L et al (2007) Inactivation of YAP oncoprotein by the Hippo pathway is involved in cell contact inhibition and tissue growth control. *Genes Dev* 21: 2747–2761

4. Zhao B, Li L, Tumaneng K, Wang CY, Guan KL (2010) A coordinated phosphorylation by Lats and CK1 regulates YAP stability through SCF(β-TTCP1). *Genes Dev* 24: 72–85
5. Hao Y, Chun A, Cheung K, Rashidi B, Yang X (2008) Tumor suppressor LATS1 is a negative regulator of oncogene YAP. *J Biol Chem* 283: 5496–5509
6. Lei QY, Zhang H, Zhao B, Zha ZY, Bai F, Pei XH, Zhao S, Xiong Y, Guan KL (2008) TAZ promotes cell proliferation and epithelial-mesenchymal transition and is inhibited by the hippo pathway. *Mol Cell Biol* 28: 2426–2436
7. Oka T, Mazack V, Sudol M (2008) Mst2 and Lats kinases regulate apoptotic function of Yes kinase-associated protein (YAP). *J Biol Chem* 283: 27534–27546
8. Huang J, Wu S, Barrera J, Matthews K, Pan D (2005) The Hippo signaling pathway coordinately regulates cell proliferation and apoptosis by inactivating Yorkie, the *Drosophila* Homolog of YAP. *Cell* 122: 421–434
9. Zhang N, Bai H, David KK, Dong J, Zheng Y, Cai J, Giovannini M, Liu P, Anders RA, Pan D (2010) The Merlin/NF2 tumor suppressor functions through the YAP oncoprotein to regulate tissue homeostasis in mammals. *Dev Cell* 19: 27–38
10. Yu FX, Luo J, Mo JS, Liu G, Kim YC, Meng Z, Zhao L, Peyman G, Ouyang H, Jiang W et al (2014) Mutant Gq/11 promote uveal melanoma tumorigenesis by activating YAP. *Cancer Cell* 25: 822–830
11. Feng X, Degese MS, Iglesias-Bartolome R, Vaque JP, Molinolo AA, Rodrigues M, Zaidi MR, Ksander BR, Merlino G, Sodhi A et al (2014) Hippo-independent activation of YAP by the GNAQ uveal melanoma oncogene through a trio-regulated rho GTPase signaling circuitry. *Cancer Cell* 25: 831–845
12. Zender L, Spector MS, Xue W, Flemming P, Cordon-Cardo C, Silke J, Fan ST, Luk JM, Wigler M, Hannon GJ et al (2006) Identification and validation of oncogenes in liver cancer using an integrative oncogenomic approach. *Cell* 125: 1253–1267
13. Moroishi T, Hansen CG, Guan KL (2015) The emerging roles of YAP and TAZ in cancer. *Nat Rev Cancer* 15: 73–79
14. Lee KP, Lee JH, Kim TS, Kim TH, Park HD, Byun JS, Kim MC, Jeong WI, Calvisi DF, Kim JM et al (2010) The Hippo-Salvador pathway restrains hepatic oval cell proliferation, liver size, and liver tumorigenesis. *Proc Natl Acad Sci USA* 107: 8248–8253
15. Camargo FD, Gokhale S, Johnnidis JB, Fu D, Bell GW, Jaenisch R, Brummelkamp TR (2007) YAP1 increases organ size and expands undifferentiated progenitor cells. *Curr Biol* 17: 2054–2060
16. Dong J, Feldmann G, Huang J, Wu S, Zhang N, Comerford SA, Gayyed MF, Anders RA, Maitra A, Pan D (2007) Elucidation of a universal size-control mechanism in *Drosophila* and mammals. *Cell* 130: 1120–1133
17. Lu L, Li Y, Kim SM, Bossuyt W, Liu P, Qiu Q, Wang Y, Halder G, Finegold MJ, Lee JS et al (2010) Hippo signaling is a potent *in vivo* growth and tumor suppressor pathway in the mammalian liver. *Proc Natl Acad Sci USA* 107: 1437–1442
18. Schlegelmilch K, Mohseni M, Kirak O, Pruszk J, Rodriguez JR, Zhou D, Kreger BT, Vasioukhin V, Avruch J, Brummelkamp TR et al (2011) Yap1 acts downstream of alpha-catenin to control epidermal proliferation. *Cell* 144: 782–795
19. Song H, Mak KK, Topol L, Yun K, Hu J, Garrett L, Chen Y, Park O, Chang J, Simpson RM et al (2010) Mammalian Mst1 and Mst2 kinases play essential roles in organ size control and tumor suppression. *Proc Natl Acad Sci USA* 107: 1431–1436
20. Zhou D, Conrad C, Xia F, Park JS, Payer B, Yin Y, Lauwers GY, Thasler W, Lee JT, Avruch J et al (2009) Mst1 and Mst2 maintain hepatocyte quiescence and suppress hepatocellular carcinoma development through inactivation of the Yap1 oncogene. *Cancer Cell* 16: 425–438
21. Atkins M, Potier D, Romanelli L, Jacobs J, Mach J, Hamaratoglu F, Aerts S, Halder G (2016) An ectopic network of transcription factors regulated by hippo signaling drives growth and invasion of a malignant tumor model. *Curr Biol* 26: 2101–2113
22. Zhao B, Ye X, Yu J, Li L, Li W, Li S, Lin JD, Wang CY, Chinnaiyan AM, Lai ZC et al (2008) TEAD mediates YAP-dependent gene induction and growth control. *Genes Dev* 22: 1962–1971
23. Overholtzer M, Zhang J, Smolen GA, Muir B, Li W, Sgroi DC, Deng CX, Brugge JS, Haber DA (2006) Transforming properties of YAP, a candidate oncogene on the chromosome 11q22 amplicon. *Proc Natl Acad Sci USA* 103: 12405–12410
24. Qiao Y, Chen J, Lim YB, Finch-Edmondson ML, Seshachalam VP, Qin L, Jiang T, Low BC, Singh H, Lim CT et al (2017) YAP regulates actin dynamics through ARHGAP29 and promotes metastasis. *Cell Rep* 19: 1495–1502
25. Zhao B, Li L, Wang L, Wang CY, Yu J, Guan KL (2012) Cell detachment activates the Hippo pathway via cytoskeleton reorganization to induce anoikis. *Genes Dev* 26: 54–68
26. Tan SM (2012) The leucocyte beta2 (CD18) integrins: the structure, functional regulation and signalling properties. *Biosci Rep* 32: 241–269
27. Chan SW, Lim CJ, Huang C, Chong YF, Gunaratne HJ, Hogue KA, Blackstock WP, Harvey KF, Hong W (2011) WW domain-mediated interaction with Wbp2 is important for the oncogenic property of TAZ. *Oncogene* 30: 600–610
28. Zhao B, Kim J, Ye X, Lai ZC, Guan KL (2009) Both TEAD-binding and WW domains are required for the growth stimulation and oncogenic transformation activity of yes-associated protein. *Cancer Res* 69: 1089–1098
29. Tapon N, Harvey KF, Bell DW, Wahrer DC, Schiripo TA, Haber DA, Hariharan IK (2002) Salvador Promotes both cell cycle exit and apoptosis in *Drosophila* and is mutated in human cancer cell lines. *Cell* 110: 467–478
30. Muller WA (2011) Mechanisms of leukocyte transendothelial migration. *Annu Rev Pathol* 6: 323–344
31. Shaw SK, Ma S, Kim MB, Rao RM, Hartman CU, Froio RM, Yang L, Jones T, Liu Y, Nusrat A et al (2004) Coordinated redistribution of leukocyte LFA-1 and endothelial cell ICAM-1 accompany neutrophil transmigration. *J Exp Med* 200: 1571–1580
32. Zhang K, Chen J (2012) The regulation of integrin function by divalent cations. *Cell Adh Migr* 6: 20–29
33. Reymond N, d'Agua BB, Ridley AJ (2013) Crossing the endothelial barrier during metastasis. *Nat Rev Cancer* 13: 858–870
34. Hohenauer T, Moore AW (2012) The Prdm family: expanding roles in stem cells and development. *Development* 139: 2267–2282
35. Wu H, Mathioudakis N, Diagouraga B, Dong A, Dombrovski L, Baudat F, Cusack S, de Massy B, Kadlec J (2013) Molecular basis for the regulation of the H3K4 methyltransferase activity of PRDM9. *Cell Rep* 5: 13–20
36. Cancer Genome Atlas Research N (2015) The molecular taxonomy of primary prostate cancer. *Cell* 163: 1011–1025
37. Prensner JR, Iyer MK, Balbin OA, Dhanasekaran SM, Cao Q, Brenner JC, Laxman B, Asangani IA, Grasso CS, Kominsky HD et al (2011) Transcriptome sequencing across a prostate cancer cohort identifies PCAT-1, an unannotated lincRNA implicated in disease progression. *Nat Biotechnol* 29: 742–749
38. Iyer MK, Niknafs YS, Malik R, Singhal U, Sahu A, Hosono Y, Barrette TR, Prensner JR, Evans JR, Zhao S et al (2015) The landscape of long noncoding RNAs in the human transcriptome. *Nat Genet* 47: 199–208

39. Robinson D, Van Allen EM, Wu YM, Schultz N, Lonigro RJ, Mosquera JM, Montgomery B, Taplin ME, Pritchard CC, Attard G *et al* (2015) Integrative clinical genomics of advanced prostate cancer. *Cell* 161: 1215–1228
40. Beltran H, Rickman DS, Park K, Chae SS, Sboner A, MacDonald TY, Wang Y, Sheikh KL, Terry S, Tagawa ST *et al* (2011) Molecular characterization of neuroendocrine prostate cancer and identification of new drug targets. *Cancer Discov* 1: 487–495
41. Enzo E, Santinon G, Pocaterra A, Aragona M, Bresolin S, Forcato M, Grifoni D, Pession A, Zanconato F, Guzzo G *et al* (2015) Aerobic glycolysis tunes YAP/TAZ transcriptional activity. *EMBO J* 34: 1349–1370
42. Bogani D, Morgan MA, Nelson AC, Costello I, McGouran JF, Kessler BM, Robertson EJ, Bikoff EK (2013) The PR/SET domain zinc finger protein Prdm4 regulates gene expression in embryonic stem cells but plays a nonessential role in the developing mouse embryo. *Mol Cell Biol* 33: 3936–3950
43. Hiratsuka S, Watanabe A, Aburatani H, Maru Y (2006) Tumour-mediated upregulation of chemoattractants and recruitment of myeloid cells predetermines lung metastasis. *Nat Cell Biol* 8: 1369–1375
44. Psaila B, Lyden D (2009) The metastatic niche: adapting the foreign soil. *Nat Rev Cancer* 9: 285–293
45. Zhao B, Li L, Lu Q, Wang LH, Liu CY, Lei Q, Guan KL (2011) Angiomotin is a novel Hippo pathway component that inhibits YAP oncoprotein. *Genes Dev* 25: 51–63
46. Wang W, Huang J, Chen J (2011) Angiomotin-like proteins associate with and negatively regulate YAP1. *J Biol Chem* 286: 4364–4370
47. Yagi R, Chen LF, Shigesada K, Murakami Y, Ito Y (1999) A WW domain-containing yes-associated protein (YAP) is a novel transcriptional co-activator. *EMBO J* 18: 2551–2562
48. Strano S, Munarriz E, Rossi M, Castagnoli L, Shaul Y, Sacchi A, Oren M, Sudol M, Cesareni G, Blandino G (2001) Physical interaction with Yes-associated protein enhances p73 transcriptional activity. *J Biol Chem* 276: 15164–15173
49. Omerovic J, Puggioni EM, Napoletano S, Visco V, Fraioli R, Frati L, Gulino A, Alimandi M (2004) Ligand-regulated association of ErbB-4 to the transcriptional co-activator YAP65 controls transcription at the nuclear level. *Exp Cell Res* 294: 469–479
50. Komuro A, Nagai M, Navin NE, Sudol M (2003) WW domain-containing protein YAP associates with ErbB-4 and acts as a co-transcriptional activator for the carboxyl-terminal fragment of ErbB-4 that translocates to the nucleus. *J Biol Chem* 278: 33334–33341
51. Zhi X, Zhao D, Zhou Z, Liu R, Chen C (2012) YAP promotes breast cell proliferation and survival partially through stabilizing the KLF5 transcription factor. *Am J Pathol* 180: 2452–2461
52. Alarcon C, Zaromytidou AI, Xi Q, Gao S, Yu J, Fujisawa S, Barlas A, Miller AN, Manova-Todorova K, Macias MJ *et al* (2009) Nuclear CDKs drive Smad transcriptional activation and turnover in BMP and TGF-beta pathways. *Cell* 139: 757–769
53. Bora-Singhal N, Nguyen J, Schaal C, Perumal D, Singh S, Coppola D, Chellappan S (2015) YAP1 regulates OCT4 activity and SOX2 expression to facilitate self-renewal and vascular mimicry of stem-like cells. *Stem Cells* 33: 1705–1718
54. Dhananjayan SC, Ramamoorthy S, Khan OY, Ismail A, Sun J, Slingerland J, O'Malley BW, Nawaz Z (2006) WW domain binding protein-2, an E6-associated protein interacting protein, acts as a coactivator of estrogen and progesterone receptors. *Mol Endocrinol* 20: 2343–2354
55. Qing Y, Yin F, Wang W, Zheng Y, Guo P, Schozer F, Deng H, Pan D (2014) The Hippo effector Yorkie activates transcription by interacting with a histone methyltransferase complex through NcoA6. *Elife* 3: e02564
56. Oh H, Slattery M, Ma L, White KP, Mann RS, Irvine KD (2014) Yorkie promotes transcription by recruiting a histone methyltransferase complex. *Cell Rep* 8: 449–459
57. Asaoka Y, Hata S, Namae M, Furutani-Seiki M, Nishina H (2014) The Hippo pathway controls a switch between retinal progenitor cell proliferation and photoreceptor cell differentiation in zebrafish. *PLoS One* 9: e97365
58. Chittka A, Nitarska J, Grazini U, Richardson WD (2012) Transcription factor positive regulatory domain 4 (PRDM4) recruits protein arginine methyltransferase 5 (PRMT5) to mediate histone arginine methylation and control neural stem cell proliferation and differentiation. *J Biol Chem* 287: 42995–43006
59. Lian I, Kim J, Okazawa H, Zhao J, Zhao B, Yu J, Chinnaiyan A, Israel MA, Goldstein LS, Abujarour R *et al* (2010) The role of YAP transcription coactivator in regulating stem cell self-renewal and differentiation. *Genes Dev* 24: 1106–1118
60. Cao X, Pfaff SL, Gage FH (2008) YAP regulates neural progenitor cell number via the TEA domain transcription factor. *Genes Dev* 22: 3320–3334
61. Morin-Kensicki EM, Boone BN, Howell M, Stonebraker JR, Teed J, Alb JG, Magnuson TR, O'Neal W, Milgram SL (2006) Defects in yolk sac vasculogenesis, chorioallantoic fusion, and embryonic axis elongation in mice with targeted disruption of Yap65. *Mol Cell Biol* 26: 77–87
62. Yan Z, Xiong Y, Xu W, Li M, Cheng Y, Chen F, Ding S, Xu H, Zheng G (2012) Identification of recurrence-related genes by integrating microRNA and gene expression profiling of gastric cancer. *Int J Oncol* 41: 2166–2174
63. Uhlen M, Zhang C, Lee S, Sjostedt E, Fagerberg L, Bidkhori G, Benfeitas R, Arif M, Liu Z, Edfors F *et al* (2017) A pathology atlas of the human cancer transcriptome. *Science* 357: eaan2507
64. Sudol M, Shields DC, Farooq A (2012) Structures of YAP protein domains reveal promising targets for development of new cancer drugs. *Semin Cell Dev Biol* 23: 827–833
65. Drbal K, Angelisova P, Hilgert I, Cerny J, Novak P, Horejsi V (2001) A proteolytically truncated form of free CD18, the common chain of leukocyte integrins, as a novel marker of activated myeloid cells. *Blood* 98: 1561–1566
66. Chen J, Yang W, Kim M, Carman CV, Springer TA (2006) Regulation of outside-in signaling and affinity by the beta2 I domain of integrin alphaLbeta2. *Proc Natl Acad Sci USA* 103: 13062–13067
67. Grossman RL, Heath AP, Ferretti V, Varmus HE, Lowy DR, Kibbe WA, Staudt LM (2016) Toward a shared vision for cancer genomic data. *N Engl J Med* 375: 1109–1112